Int. J. Electrochem. Sci., 7 **(2012)** 10164 - 10174

International Journal of
ELECTROCHEMICAL
SCIENCE
www.electrochemsci.org

Effect of Stresses for Electrochemical Calculations of Mg-Zn-In-Sn Alloy

Zhan Yu[1], *Dongying Ju*[2, 3, *], *Takashi Nukii*[4]

[1] Graduate School of Saitama Institute of Technology, Fusaiji 1690, Fukaya, Saitama 369-0293, Japan
[2] Department of Material Science and Engineering, Saitama Institute of Technology, Fusaiji 1690, Fukaya, Saitama 369-0293, Japan
[3] Department of Material Science and Engineering, University of Science and Technology Liaoning, Anshan 114051, China
[4] Engineering Development Center of Atox, Kasiwa1201, Tiba 277-0861, Japan
[*]E-mail: dyju@sit.ac.jp

Received: 27 July 2012 / *Accepted:* 20 August 2012 / *Published:* 1 October 2012

A potential model has been developed for calculating electrochemical potential data for Mg alloy Mg-Zn-In-Sn with stresses immersed in 3.5% NaCl solution. Open circuit potential (OCP)s and loop current (LC)s are calculated by the concentrations of Mg^{2+}, which are measured via inductively coupled plasma (ICP) analysis and FACSIMILE software simulation. The results investigate that the calculated results of OCPs and LCs were mainly consistent with the experimental results. The corrosion mechanism of Mg-Zn-In-Sn alloy is revealed on the theoretial, and the infuence of stresses on the alloy anode is investigated in the paper.

Keywords: Mg-Zn-In-Sn alloy; Simulation; Calculation; Electrochemical corrosion behavior

1. INTRODUCTION

The importance of Mg alloys has increased significantly in various industries due to the high strength/weight ratio, high dimensional stability, good machining, and ability to recycled [1]. Moreover, the employment of Mg as an anodic material in different types of batteries has been paid much attention in recent years [2]. Among Mg alloys, AZ91 is one of those having the best mechanical properties/corrosion behaviour balance [3]. Therefore, we have recently developed a new Mg alloy anode material called Mg-Zn-In-Sn alloy by adding the elements Zn, In and Sn into commercial Mg alloy AZ91 [4]. Mg-Zn-In-Sn alloy anode has more negative OCP and higher LC than those of AZ91 alloy because of the addition of elements [5]. Furthermore, effects of stress on the electrochemical corrosion behaviours of Mg-Zn-In-Sn alloy anode were evaluated in our previously studies [6]. However, the corrosion mechanisms of Mg alloys are very complicated and much is still unknown, which justifies the importance of Mg alloys to increase the understanding of the processes involved gradually. Therefore, the voltage and current studies aim to reveal the corrosion processes and electrochemical properties of Mg-Zn-In-Sn alloy anode with stresses of 0, 5, 10, 50, 100 MPa. In this paper, OCPs and LCs are calculated by the concentrations of Mg^{2+}, which are measured via inductively coupled plasma (ICP) analysis and FACSIMILE software simulation. FACSIMILE software is a very efficient robust and versatile suite of closely related computer programs for the modeling of complex dynamic chemical reactions. Therefore the reaction rates of Mg and water under stress corrosion are calculated via the results of ICP measurement. And FACSIMILE software is used to simulate the Mg^{2+} concentration variations by the reaction rates during stress corrosion for 1h in our research. Simultaneously, Tafel factors are investigated to confirm the influence of stress on the electrochemical properties of alloy anode through current curve calculation.

2. EXPERIMENTAL AND POTENTIAL MODEL

2.1 Materials

Mg-Zn-In-Sn alloy was casted via the twin-roll continuous casting method that manufactured by adding metal elements Zn (1 wt. %), In (2 wt. %), and Sn (2 wt. %) in AZ91 alloy. The alloy featured higher mechanical properties and electrochemical properties than that of AZ91 alloy [4, 5]. The chemical composition of Mg-Zn-In-Sn alloy is shown in Table 1. Specimens made of Mg-Zn-In-Sn alloy sheets by a wire cutting apparatus (Mitsubishi Electric Corporation W11FX2K) were used in the stress corrosion measurements.

Table 1. Chemical composition of Mg-Zn-In-Sn alloy

Material	Chemical composition, wt. %						
	Al	Zn	In	Sn	Mn	Other total	Mg
Mg-Zn-In-Sn	10.161	0.776	0.877	1.847	0.268	0.138	balance

2.2 Mg^{2+} concentrations measurement and simulation

The electrochemical corrosion experiments with stresses of 0 (non-stress), 5, 10, 50, and 100 MPa, were carried out in 3.5 wt.% NaCl solution for 1 h at room temperature. Concentrations measurements of Mg^{2+} in the corrosion solution were performed by ICP (ICPS-7000, SHIMADSU).

The standard curve of Mg^{2+} concentration is shown in Figure 1, which is drawn via standard Mg^{2+} solution measurement with the Mg^{2+} concentration of 0, 1, 2, 5 and 10 mg/L, presented by Equation 1.

$$y = 0.0593986x + 0.002884 \tag{1}$$

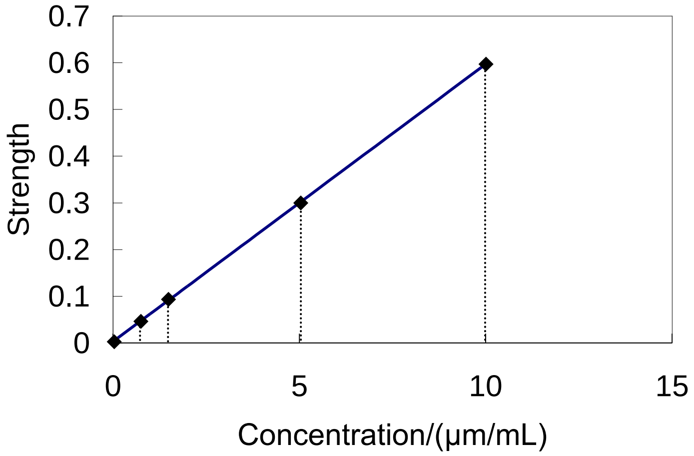

Figure 1. Standard curve of Mg^{2+} concentration in 3.5% NaCl solution

Base on the standard curve, Mg^{2+} concentrations were measured under stresses corrosion. And then the variations of Mg^{2+} concentration were simulated by FACSIMILE software during 1 h with the reaction rate calculated by the Mg^{2+} concentration measurements.

2.3 Electrochemical model calculation

The Mg alloy corrosion reaction follows overall equation:

$$Mg(s) + 2H_2O(l) \rightarrow Mg(OH)_2(s) + H_2(g) \tag{2}$$

The simplified equation can be broken down into the cathodic (Eq. 3), anodic (Eq. 4) partial reactions and product reaction (Eq. 5):

$$2H_2O + 2e^- \rightarrow H_2 \uparrow + 2OH^- \tag{3}$$

$$Mg \rightarrow Mg^{2+} + 2e^- \tag{4}$$

$$Mg^{2+} + 2OH^- \rightarrow Mg(OH)_2 \downarrow \tag{5}$$

The reaction rate was calculated by ICP values, and variations of Mg^{2+} concentrations were simulated by FACSIMILE software [7]. OCP and LC calculation model was based on the values of reaction rate and the variation of Mg^{2+} concentrations. And then the calculation values of OCPs and

LCs were compared with the experiment values and the relationship between the stress and the anodic Tafel constant was discussed.

3. RESULTS AND DISCUSSION

3.1 Mg2+ concentration variation

The Mg^{2+} concentrations in the corrosion solution after 1 h stress corrosion were measured as shown in Table 2. The results investigate that product reactions of Mg-Zn-In-Sn alloy anode are promoted by the effect of stresses. The concentrations of Mg^{2+} in the corrosion solution decrease with the increasing of stresses. And the variation of concentrations directly affects OCP values of Mg-Zn-In-Sn alloy anode through the Nernst equation, later discussed in this paper.

Table 2. Mg^{2+} concentration values after stress corrosion

Stress (MPa)	0	5	10	50	100
Mg2+ concentration(mol/L)	0.03531	0.00587	0.00442	0.00309	0.00195

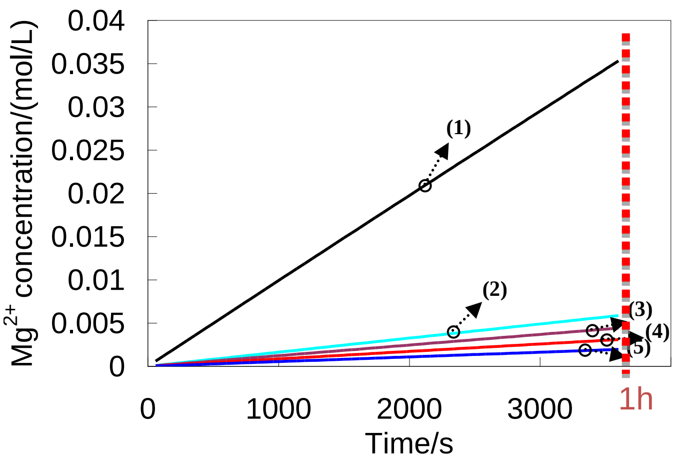

Figure 2. Mg^{2+} concentration simulated curves of Mg-Zn-In-Sn alloy anode under stress corrosion (1) 0 MPa; (2) 5 MPa; (3) 10 MPa; (4) 50 MPa; (5) 100 MPa

And the Mg^{2+} concentrations during 1 h are simulated by FACSIMILE software, as shown in Fig. 2. The inclinations of lines reveal that the reaction rates of corrosion increase with the increasing of stresses. Therefore, the results investigate that corrosion reactions are promoted by the effect of stress.

3.2 OCP calculation

The applied stress energy improved the electrochemical potentials of alloy anode, and persisted together with stresses, because the stresses did not exceed the elastic limit. The change in free energy ΔG (per g) is given by Equation (6):

$$\Delta G = \frac{\sigma^2}{2\rho Y} \tag{6}$$

where σ is the applied stress, Y is Young's modulus, and ρ is the density of the Mg-Zn-In-Sn alloy. The free energy of Mg-Zn-In-Sn alloy anode increased as the applied stresses increased. The negative removal of voltage ΔE was calculated with the change in energy using Equation (7).

$$\Delta E = -\frac{\Delta G}{nF} \tag{7}$$

where n is the number of moles of electrons transferred and F is the Faraday constant. As the energy increased, the OCPs of the alloy anodes were negatively removed. The stresses are investigated to determine the OCP values of Mg-Zn-In-Sn alloy anode. However, the concrete values of OCP are not easy to calculated by variations of free energy [8]. Therefore, the simulated Mg^{2+} concentrations values are used to calculate the OCP values of Mg-Zn-In-Sn alloy anode by the Nernst equation.

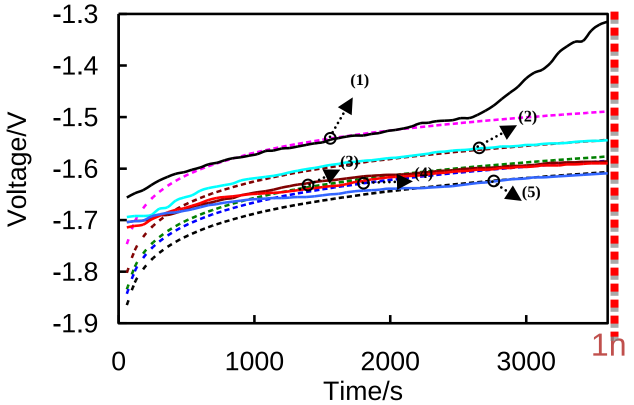

Figure 3. Comparison of OCP curves for Mg-Zn-In-Sn alloy anode under stress corrosion (1) 0 MPa; (2) 5 MPa; (3) 10 MPa; (4) 50 MPa; (5) 100 MPa

The OCPs were calculated by the following Equations (8).

$$E = E_0 + \frac{RT}{nF} \ln \frac{[O_x]}{[R_{ed}]} \tag{8}$$

where E_0 is the equilibrium potential for this reaction, F is Faraday constant, R is gas constant, $[O_x]$ is the concentration of oxidant, and [Red] is the concentration of reductant. The calculation values of OCP are consistent with experimental results as shown in Fig. 3. However, the experimetal OCP value of Mg-Zn-In-Sn alloy anode has obvious positive removal from about 40 min, which is not consistent with the calculation value of OCP. This finding can be attributed to the interference of environmental factors, such as the forming of corrosion product film and pH value of solution [9].

3.3 LC calculation

The LCs were calculated by introducing correction factor A to modify the expression of corrosion current density [1]. Therefore, the LC density was expressed using Equations (9) and (10):

$$i = \frac{[e^{(|E|-E_0)/b_a} - e^{-(|E|-E_0)/b_c}]}{[1/Ai_0 + x]} \tag{9}$$

and

$$x = \frac{e^{(|E|-E_0)/b_a}}{Ai_0 \exp[0.523(|E|-E_0)^5]} \tag{10}$$

where i_0 is the experimental current density, b_a and b_c are the anodic and cathodic Tafel factors, respectively, and E_0 is the equilibrium potential for this reaction, as computed from the Nernst equation. The LCs were calculated by Equation (11) in this paper. The LCs were calculated by introducing correction factor A to modify the expression of corrosion current density.

$$i = \frac{Ai_0 \exp[0.523(|E|-E_0)^5]\{\exp[(|E|-E_0)/b_a] - \exp[-(|E|-E_0)/b_c]\}}{\exp[0.523(|E|-E_0)^5] + \exp[(|E|-E_0)/b_a]} \tag{11}$$

where i_0 is the experimental current density, b_a and b_c are the anodic and cathodic Tafel constants, and E_0 is the equilibrium potential for this reaction as computed from the Nernst equation, respectively.

Values for the various parameters are given in Table 3. Using equation (11), the current densities are calculated density under different stress corrosion conditions of 0, 5, 10, 50 and 100MPa, respectively. And the LCs are calculated by the equation (12).

$$I = S \times i \tag{12}$$

where *I* is the calculation current, S is the surface area of alloy anode.

Equations (11) and (12) were developed empirically and provide a reasonable representation of experimental results. By adjusting the Tafel factors, the calculated results were mainly consistent with the experimental results. Comparisons of the current curves between experimental and calculated values are shown in Fig. 4. Therefore, as shown in Table 3, the stresses have effects on the changes in the anodic Tafel factors. The Tafel factors become bigger as stresses increased, and the LC values also improved as the Tafel factors increased. The modified model of the LC verifies the reliability of experimental results [10-12].

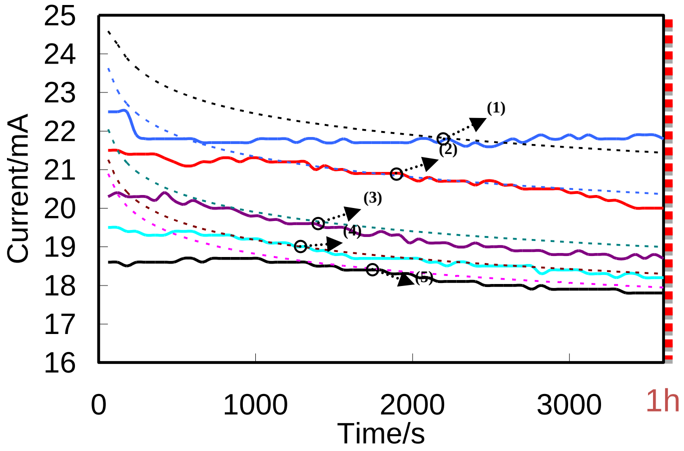

Figure 4. Comparison of LC curves for Mg-Zn-In-Sn alloy anode under stress corrosion (1) 0 MPa; (2) 5 MPa; (3) 10 MPa; (4) 50 MPa; (5) 100 Mpa

Table 3. Values for Parameters for the LCs

No.	i_p^0 (A/m^2)	b_a (V)	b_c (V)	E_0 (V)	A
1. 0MPa	0.541	1.690	0.060	-2.37	10
2. 5MPa	0.556	1.720			
3. 10MPa	0.574	1.730			
4. 50MPa	0.617	1.735			
5. 100MPa	0.645	1.740			

3.4 Morphologies of Mg-Zn-In-Sn alloy anodes after stress corrosion

The surface and cross section morphologies of alloy anode were observed after electrochemical measurement experiments with non-stress corrosion and stresses corrosion of 5 to 100 MPa were performed for 1 h. The surface morphology of specimen with non-stress was uniformly covered with the corrosion product film as shown in Fig. 5a.

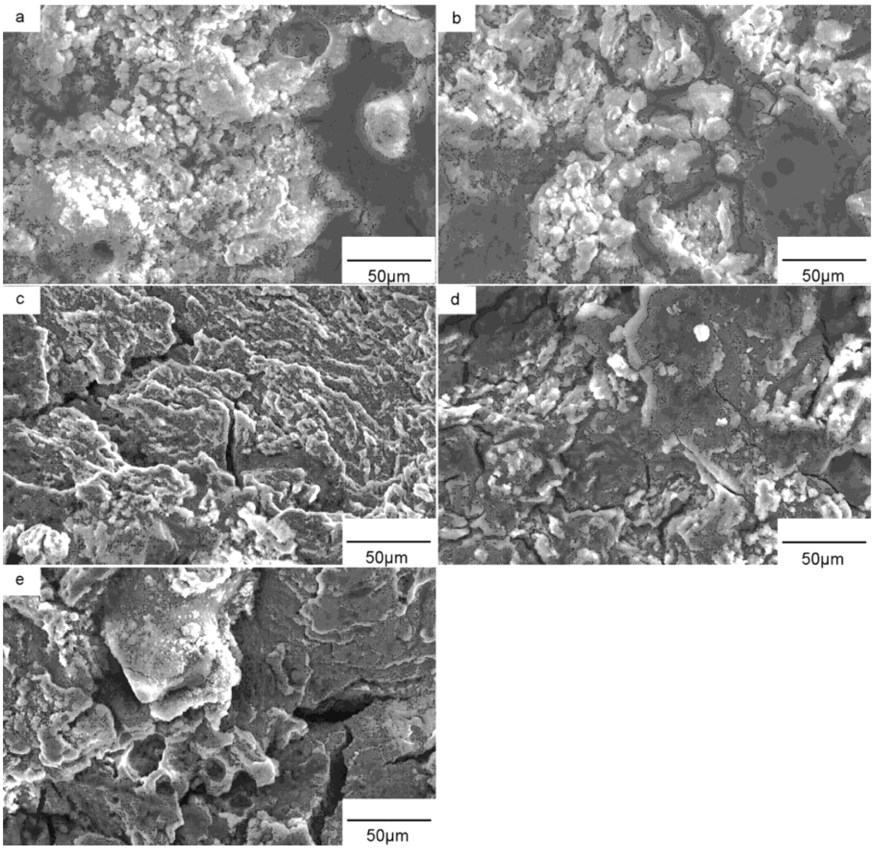

Figure 5. SEM image of stress corrosion surface morphology (a) 0 MPa; (b) 5 MPa; (c) 10 MPa; (d) 50 MPa; (e) 100 Mpa

The corrosion reaction between alloy anode and NaCl solution was hindered by forming of the film. Therefore, the OCPs of alloy anodes had an apparently positive removal as experiment progressed, discussed in the former paper. Because the calculation result of OCP is base on the Mg^{2+} concentrations in the solution, from about 40 min, the calculated value is not consistent with experimental value by the influence of film. However, applied stresses promoted electrochemical activities of alloys, the corrosion product films on the specimens became easy to shed off as shown in Figures 5b–5e. The resistance between NaCl solution and alloy anode decreased, which promoted the electrochemical corrosion reaction. As shown in Fig. 5b, the surface of alloy anode was almost covered with the corrosion film with a few light cracks. The contact area of Mg and water increases, the product reaction is promoted by effect of stress, obviously. Therefore, the concentrations of Mg^{2+} decrease by the applied stress. And OCP with stress of 5 MPa was more negative, and LC became higher than that with non-stress. As shown in Figures. 5c–5e, the corrosion product films were shed off intensively by the effect of stresses, and numerous cracks appeared on the films. Consequently, Mg^{2+} concentrations in the corrosion solution decrease with the increasing of stresses investigated by ICP values, and OCPs of alloy anodes had negative removals and LCs of alloy anodes improved obviously due to influence of the applied stresses [13, 14].

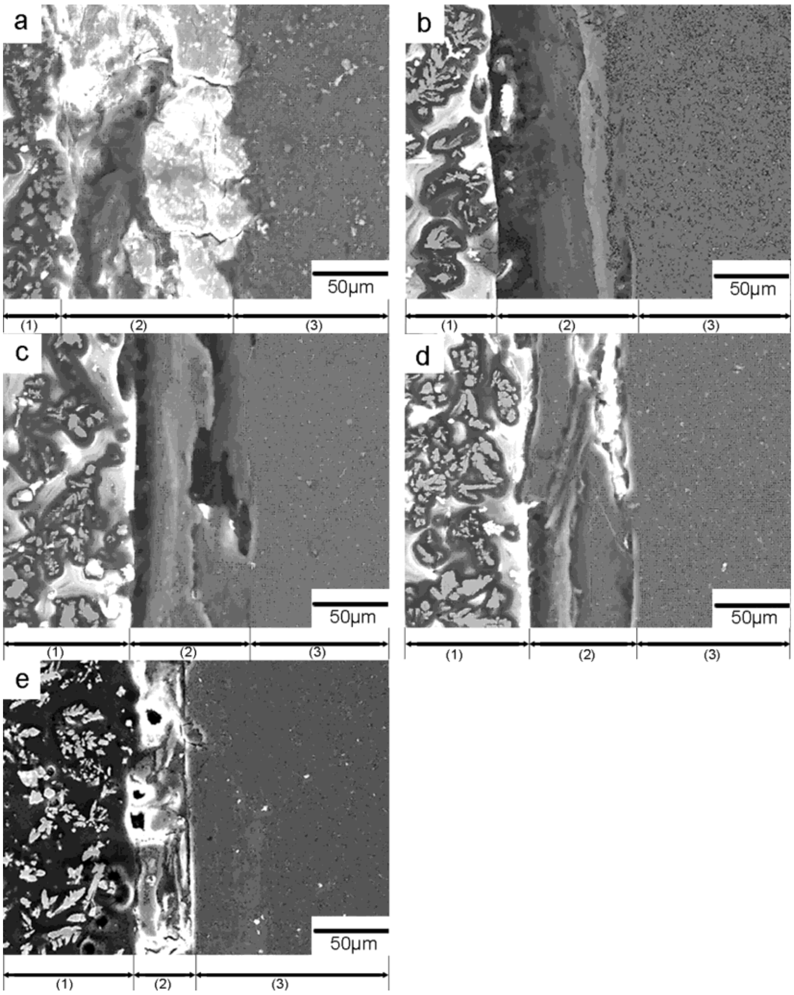

Figure 6. SEM image of stress corrosion cross section morphology (1) conductive resin, (2) corrosion product layer, (3) alloy matrix (a) 0 MPa; (b) 5 MPa; (c) 10 MPa; (d) 50 MPa; (e) 100 MPa

Figures. 6a-6e show the cross section morphologies of alloy anodes after stress corrosion with a conductive resin on the left-hand side, the corrosion product film in the middle and not corroded part of the alloy matrix on the right-hand area . The thickness of corrosion product film was approximately 80 μm with non-stress (Fig. 6a). The thickness of the film decreased to approximately 50 μm with the applied stress of 5 MPa (Fig. 6b). The thickness of the film deceased to 30 μm and did not change significantly with stresses of 10, 50, and 100 MPa, as shown in Figs. 6c-6e. Subsequently, the concentrations of Mg^{2+} decrease with the increasing of stresses. This result indicates that the electrochemical corrosion reactions between Mg-Zn-In-Sn alloy and NaCl solution progressed smoothly, and the Mg^{2+} concentration in the corrosion solution decrease by the effect of stress. Therefore, higher electrochemical potential of alloy anode could be obtained by stress corrosion. However, with stresses of 10, 50, and 100 MPa, the thicknesses of the corrosion product films had no evident changes with the increasing of stresses. The OCP values had no significantly negative removal with these stresses, neither, as discussed in the above results. And the calculated OCP and LC values are well consistent with the changing of experimental results [15, 16].

4. CONCLUSIONS

This paper determined a potential model developed for calculating electrochemical potential data for Mg alloy Mg-Zn-In-Sn with stresses immersed in 3.5% NaCl solution. Furthermore, the OCPs and LCs were calculated by the electrochemical potential model, in order to reveal the effect of stresses.

1. The concentrations of Mg^{2+} in the corrosion solution decrease with the inceasing of stresses.
2. The corrosion product films on the surface of specimen became easy to shed off due to the applied stresses. The resistance between NaCl solution and alloy anode decreased, which promoted the electrochemical corrosion reaction.
3. In general, the thicknesses of corrosion product films on alloy anodes surface decreased as the applied stresses increased. However, the thicknesses of corrosion product films with stresses above 10 MPa did not decrease significantly. This phenomenon explains the variation of OCP values of alloy anode because of the influence of experimental factors.
4. The calculation values of OCP are almostly consistent with experimental results. The difference between calculation values and experiment values can be attributed to the interference of environmental factors, such as the forming of corrosion product film. The corrosion mechanism of Mg-Zn-In-Sn alloy is revealed on the theoretial, and the infuence of stresses on the alloy anode is investigated.
5. By adjusting the Tafel factors, the LC calculation results were mainly consistent with the experimental results. The modification of Tafel constants also demonstrated the effct of applied stresses on the theoretial.

ACKNOWLEDGEMENTS
This work was partially supported by the “Nano Project” for Private Universities: 2011-2014 matching fund subsidy from Ministry of Education, Culture, Sports, Science and Technology.

References

1. D. D. Macdonald, Science. 48 (1992): 194.
2. F. H. Cao, V. H. Len, Z. Zhang and J. Q. Zhang, *Russian J. Electrochem.*. 43 (2007): 878.
3. T. D.Gregory, R. J. Hoffman and R. C. Winterton, *J. Electrochem. Soc*. 137 (1990): 775
4. Z. Yu, D. Y. Ju, H. Y. Zhao, and X. D. Hu, *J. Environ. Sci.* 23 (2011): 95.
5. Z. Yu, H. Y. Zhao, X. D. Hu, and D. Y. Ju, *Transactions of Nonferrous Metals Society of China*. 20 (2010): 318.
6. Z. Yu, D. Y. Ju, and H. Y. Zhao, *Int. J. Electrochem. Sci.*. in press.
7. K. Ishigure, T. Nukii, and S. Ono, *J. Nuclear Mater.*. 350 (2006): 56.
8. M. Clarke, Corrosion Science. 10 (1970): 671.
9. Y. B. Unigovski, L. Riber, and E. M. Gutman, *J. Metals, Mater. Minerals*. 17 (2007): 7.
10. T. Shibata, *J. Soc. Mater. Sci.*. 55 (2006): 979.
11. P. L. Bonora, M. Andrei, A. Eliezer and E. M. Gutman, *Corr. Sci.*. 44 (2002): 729.
12. J. Q. Wang, J. Chen, E. Han and W. Ke, *Mater. Transaction*. 49 (2008): 1052.

13. W. Walke, J. Przondziono, E. Hadasik, J. Szala and D. Kuc, *J. Achievements in Materials and Manufacturing Engineering*. 45 (2011): 132.
14. J. Orlikowski and K. Darowicki, *J. Solid State Electrochem*. 13 (2009): 1659.
15. A. Pardo, M. C. Merino, A. E. Coy, R. Arrabal, F. Viejo and E. Matykina, *Corr. Sci.* 50 (2008): 823.
16. R. G. Song, C. Blawert, W. Dietzel and A. Atrens, *Mater. Sci. Engin*. 399 (2005): 308.